



## ELECTRICAL AND THERMAL CONDUCTIVITIES OF IRON (II, III) OXIDE ADDED RIGID POLYURETHANE FOAM NANOCOMPOSITES

Meral AKKOYUN

Bursa Technical University, Faculty of Engineering and Natural Sciences, Department of Polymer Materials  
Engineering, Bursa, TURKEY  
[meral.akkoyun@btu.edu.tr](mailto:meral.akkoyun@btu.edu.tr)

(Geliş/Received: 18.09.2020; Kabul/Accepted in Revised Form: 08.12.2020)

**ABSTRACT:** Effect of iron (II, III) oxide particles on the electrical and thermal conductivities and thermal transitions of rigid polyurethane foams, and hence on the final density and microstructure of these porous materials were investigated. The microstructure study of iron (II, III) oxide added rigid polyurethane foam nanocomposites indicated a drop by 27% of the mean cell size from 294  $\mu\text{m}$  for the neat polyurethane to 215  $\mu\text{m}$  for a filler content of 50wt.% and an increase of the mean strut thickness as a function of the filler content. The thermal transition results demonstrated that as the magnetite content rises a visible decrease by 32% of the glass transition temperature appears in the case of soft segments when the glass transition temperature representing hard segments remains constant. Results of the electrical conductivity measurements showed a significant increase by 17% up to the higher filler content of 50wt.% compared to the unfilled polyurethane foam. The thermal conductivity results of iron (II, III) oxide added rigid polyurethane foam nanocomposites revealed a thermal insulating effect of magnetite particles due to the decrease of the thermal conductivity and stabilization after a slight rise from 0.02431W/m.K to 0.02648W/m.K depicted for a filler amount of 4wt.%.

**Keywords:** Rigid polyurethane foam, Iron (II, III) oxide, Thermal conductivity, Electrical conductivity

### Demir (II, III) Oksit Katkılı Rijit Poliüretan Köpük Nanokompozitlerin Elektriksel ve Termal İletkenlikleri

**ÖZ:** Demir (II, III) oksit partiküllerinin rijit poliüretan köpüklerin elektrik ve termal iletkenlikleri ile termal geçişlerine ve dolayısıyla bu gözenekli malzemelerin nihai yoğunluğu ve mikroyapısına etkisi araştırılmıştır. Demir (II, III) oksit eklenmiş rijit poliüretan köpük nanokompozitlerin mikroyapı çalışması, ortalama hücre boyutunun katkısız poliüretan için 294  $\mu\text{m}$  değerinden ağırlıkça %50 katkılı köpük için 215  $\mu\text{m}$  değerine kadar, %27 oranında bir düşüş ve katkı oranına bağlı olarak ortalama duvar kalınlığında bir artış olduğunu göstermiştir. Termal geçiş sonuçları, magnetit oranı arttıkça yumuşak segmentler için camı geçiş sıcaklığında %32 oranında gözle görülür bir düşüşün ortaya çıktığını ve sert segmentleri temsil eden camı geçiş sıcaklığının sabit kaldığını göstermiştir. Elektriksel iletkenlik ölçümlerinin sonuçları, katkısız poliüretan köpüğe kıyasla ağırlıkça %50 katkı oranına kadar %17 oranında önemli bir artış göstermiştir. Demir (II, III) oksit eklenmiş rijit poliüretan köpük nanokompozitlerin termal iletkenlik sonuçları, ağırlıkça %4 katkı oranı için 0.02431W/m.K değerinden 0.02648W/m.K değerine kadar gözlemlenen hafif bir artıştan sonra termal iletkenliğin azalması ve stabilizasyonu nedeniyle manyetit parçacıklarının ısı yalıtım etkisini ortaya çıkarmıştır.

**Anahtar Kelimeler:** Rijit poliüretan köpük, Demir (II, III) oksit, Termal iletkenlik, Elektriksel iletkenlik

## 1. INTRODUCTION

Among organic polymeric materials, polyurethanes (PU) exhibited a wide usage in various technological applications such as insulation, electronic, coatings, furnishing, and biomaterials mainly because of its relatively low manufacturing costs and facile processability (Akkoyun & Suvaci, 2016; Wilkes & Wildnauer, 1975; Sattar, et al., 2015; Usman, et al., 2016; Akkoyun & Akkoyun, 2019).

These polymeric materials can also be exploited as solid foams and depending on their cellular structure they can be categorized in two main groups: rigid foams composed of a closed cell structure and flexible foams composed of an open cell structure (Baferani, et al., 2017; Akkoyun & Akkoyun, 2019). Due to their outstanding properties and performances, the application range of these materials is quite broad and can be extended from construction, automotive to household sectors (Chattopadhyay & Webster, 2009). The distinctions between rigid and flexible PU foams give them various properties which can be designed according to the aimed utilization.

Rigid PU foams can be used in a large range of applications and particularly in construction and other industrial sectors thanks to their excellent properties such as low thermal conductivity, good sound barrier, low density, low water absorption and good dimensional stability while they present poor mechanical strength and thermal stability (Lee, et al., 2005; Saha, et al., 2005; Akkoyun & Akkoyun, 2019; Lee & Ramesh, 2004; Akkoyun & Suvaci, 2016). The desired final properties of these composites are mainly controlled by the processing conditions but also by the microstructure parameters of PU foams such as the mean cell diameter, the mean cell strut thickness, the cell density and the initial polyol and isocyanate used for the synthesis of PU foams (Saha, et al., 2008; Ibeh & Bubacz, 2008).

In the last few years, metal-oxide powders are more commonly utilized in the domain of polymers and particularly for electrotechnical devices. Magnetic particles and particularly iron (II, III) oxide ( $\text{Fe}_3\text{O}_4$ ) due to their important magnetic, mechanical and thermal properties, have attracted much attention in the preparation of rigid PU foam composites and can be used in a wide range of applications (Alavi Nikje, et al., 2015a; Alavi Nikje, et al., 2015b; Alavi Nikje, et al., 2013; Moghaddam & Naimi-Jamal, 2018; Silva, et al., 2020; Zhou, et al., 2010). Furthermore, metal-oxide added polymer composites are good candidates to replace for example metals or metal oxides in numerous applications as radio frequency interference shielding. These materials, due to their higher thermal conductivity compared to their neat counterparts are preferred in applications requiring lower sizes and improved power production (Saha, et al., 2008).

As the surface of iron (II, III) oxide particles presents low amount of functional groups, in the literature several studies were investigated for the compatibilization of these magnetic particles with different polymers (Chen, et al., 2017; Zhang, et al., 2017; Zou, et al., 2015). In the same way, the studies about iron (II, III) oxide filled rigid PU foams are mainly focused on the surface modification of magnetic particles in order to improve the properties of nanocomposites (Alavi Nikje, et al., 2015a; Alavi Nikje, et al., 2013; Alavi Nikje, et al., 2015b; Moghaddam & Naimi-Jamal, 2018). However, the electrical and thermal conductivity properties of modified iron (II, III) oxide added rigid PU foam composites were not investigated in the literature. Limited works can be found in the literature about unmodified iron (II, III) oxide added rigid PU foams (Silva, et al., 2020; Zhou, et al., 2010). Silva et al. (2020) were focused on the effect of the filler content on the attenuation of incident radiation properties of these  $\text{Fe}_3\text{O}_4$  added rigid foam nanocomposites to produce electromagnetic radiation absorbent materials. In another work, Zhou et al. (2010) studied the properties of rigid PU/ $\text{Fe}_3\text{O}_4$  foams and particularly the immobilization of microbial biomass of microorganisms in order to use these composites as carrier for wastewater treatment. As a result, the effect of unmodified  $\text{Fe}_3\text{O}_4$  powder content on the electrical and thermal conductivities of highly  $\text{Fe}_3\text{O}_4$  filled rigid PU foam were not explored yet.

The aim of this study is to use unmodified  $\text{Fe}_3\text{O}_4$  for the fabrication of iron (II, III) oxide added rigid PU foam nanocomposites and to investigate their electrical and thermal conductivities, microstructure and thermal transition properties in order to i) detect the optimum properties of these materials without surface treatment and ii) simplify the processing of these foam nanocomposites by eliminating the surface treatment step of the fillers and then reduce costs. In this work, rigid PU foams filled with iron (II, III) oxide at different concentrations were prepared using a three-step procedure (Saha, et al., 2008). All

samples were obtained by free rise method into a custom-made rectangular mold. Electrical and thermal conductivities, thermal transitions and microstructure of rigid PU foams filled with  $\text{Fe}_3\text{O}_4$  particles were investigated. The effect of the filler content on the final properties of these rigid PU foam nanocomposites was studied. Then, the relationship between these properties was examined in an attempt to identify the parameters influencing their evolution.

## 2. MATERIALS and METHODS

### 2.1. Materials

Iron (II, III) oxide powder which has an average initial particle size of about 30 nm was provided from Nanokar/Turkey. Figure 1 shows the scanning electron microscopy (SEM) image of magnetite nanoparticles. Polyol (KIMrigid RD 057) and isocyanate (Izokim RD 001) obtained from Kimteks/Turkey were used in this work. The density, NCO content and viscosity of isocyanate are respectively 30.5-32.5%, 1.23 g/cm<sup>3</sup> and 200 ± 40 mPa.s. The density and viscosity of polyol are respectively 1.03 g/cm<sup>3</sup> and 400 mPa.s.

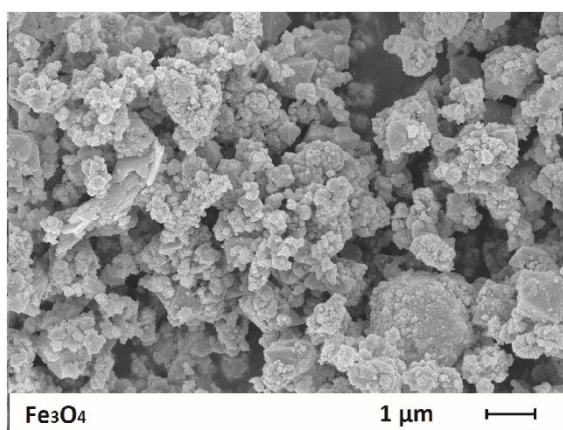


Figure 1. SEM image of Iron (II, III) oxide nanoparticles

### 2.2. Preparation of unfilled and $\text{Fe}_3\text{O}_4$ filled rigid PU foam nanocomposites

First of all, iron (II, III) oxide powder was dried at 100°C during 12 hours using an oven. PU/ $\text{Fe}_3\text{O}_4$  composites were prepared at different filler content in polyol (4, 8, 16, 32, 40 and 50wt.%). Then, during the first step of PU synthesis, the powder was added in the polyol and the polyol/ $\text{Fe}_3\text{O}_4$  blend was mixed using an ultrasonic sonicator (Bandelin, UW 3200) for 10 min in order to obtain a well dispersed suspension. In the second step, the suspension was mixed for 1 minute at 2000 rpm using a mechanical stirrer (DLAB, OS20-PRO). Then, the isocyanate was immediately added into the polyol/ $\text{Fe}_3\text{O}_4$  mixture and the stirring continued for another 5 seconds. The prepared blend was poured into an aluminum mold (30x30x4 cm) designed for this work. Then, the samples were cured at standard ambient conditions (room temperature and atmospheric pressure) during 24 hours. All sample characterizations were performed after 24 hours of curing time.

### 2.3. Characterization methods

The microstructure analyses of the unfilled and iron (II, III) oxide added rigid PU foam composites were performed with a Carl Zeiss Gemini 300 scanning electron microscope at 10 kV. A gold/palladium coating was realized for all foam samples before the measurement. SEM micrographs were recorded for foam sections perpendicular to the foaming direction. Image J software was used for the detection of cell

sizes from SEM micrographs. A mean cell diameter was calculated from 100 cells using SEM micrographs for sample sections perpendicular to the foaming direction.

Apparent density of the unfilled and iron (II, III) oxide added rigid PU foams was measured according to the ASTM D-1622 standard.

Thermal transitions of unfilled and magnetite added rigid PU foams were characterized using a TA Instrument Discovery DSC25 Differential Scanning Calorimeter (DSC) under nitrogen atmosphere. The measurements were realized in a temperature range of  $-80^{\circ}\text{C}$ - $300^{\circ}\text{C}$  and at a heating rate of  $10^{\circ}\text{C}/\text{min}$ .

The thermal conductivity measurements of unfilled and iron (II, III) oxide added rigid PU foam composites (dimensions:  $30\text{cm}\times 30\text{cm}\times 4\text{cm}$ ) were carried out using a Laser comp. Fox 314 (TA Instruments) heat flow meter according to ASTM Standard C518. Three replicates were analyzed for each sample.

The electrical conductivity of unfilled and iron (II, III) oxide added rigid PU foam composites were detected with a KEITHLEY 6517-B multimeter equipped with a resistivity test fixture (8009). Three replicates of the PU foam nanocomposites ( $3\times 3\text{cm}^2$ ) were used for the measurements.

### 3. RESULTS and DISCUSSIONS

#### 3.1. Effect of filler concentration on the microstructure of rigid PU/ $\text{Fe}_3\text{O}_4$ foam nanocomposites

SEM images of 0, 4, 8, 16, 32, 40 and 50wt.%  $\text{Fe}_3\text{O}_4$  added rigid PU/ $\text{Fe}_3\text{O}_4$  porous foam samples were given in Figure 2. The measurements were carried out for foam sections perpendicular to the foaming direction. For these samples, the structure of the cells seems to be isotropic for all filler concentrations. The average cell diameters (Figure 2) and average strut thicknesses (Figure 3) of the foams were calculated from SEM micrographs as described in Materials and Methods part. The apparent densities of the foams were also obtained and all results were gathered in Table 1.

From Figure 2 and 4 and Table 1, the mean cell diameters of rigid PU/ $\text{Fe}_3\text{O}_4$  foam nanocomposites decreases from  $294\ \mu\text{m}$  for the neat PU to  $215\ \mu\text{m}$  for a filler content of 50wt.% indicating that the mean cell diameter was diminished by 27%. These results are in correlation with those determined for nanofiller reinforced rigid PU foam nanocomposites where a drop is also observed as the nanofiller amount rises (Akkoyun & Suvaci, 2015). In addition from Figure 4 and Table 1 an increase of the cell density and the strut thickness is observed and it can be concluded that these results support the previous values detected for the cell size evolutions. Actually, as mentioned in the literature (Akkoyun & Suvaci, 2015) nanofillers allow an augmentation of the amount of the nucleation sites inducing an increase of the density and at the same time a decrease of the cell size of the foams as demonstrated in Table 1.

Figure 3 shows SEM images recorded for rigid PU/ $\text{Fe}_3\text{O}_4$  foams filled at high concentrations of magnetite (32, 40 and 50wt.%) in order to detect the dispersion state of the fillers into the PU matrix. As a result of the use of unmodified iron (II, III) oxide particles with high surface energy, SEM images revealed the presence of iron (II, III) oxide agglomerates related with the lower interactions between the particles and the polymer matrix as largely reported in the literature (Alavi Nikje, et al., 2015a; Moghaddam & Naimi-Jamal, 2018).

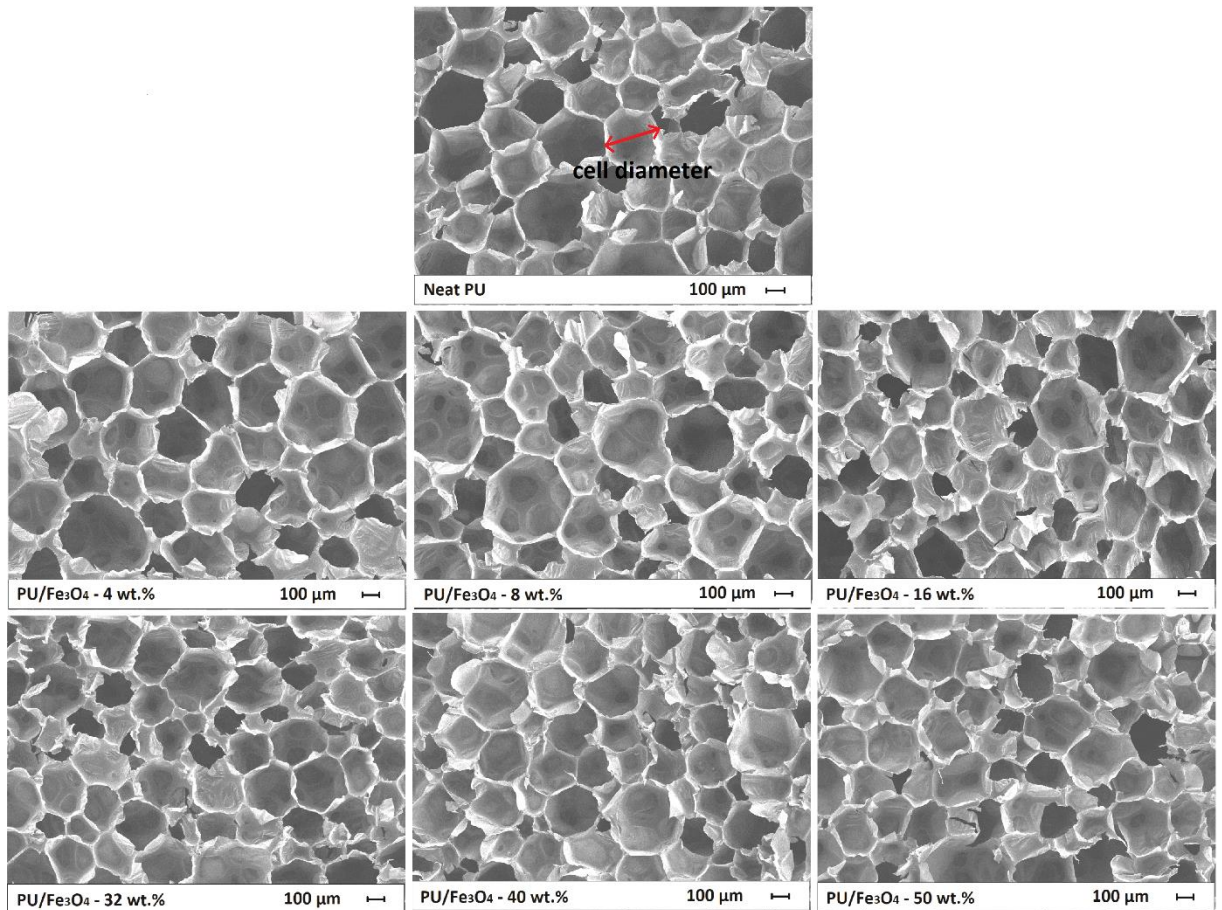


**Figure 2.** SEM images obtained for unfilled PU foam and  $\text{Fe}_3\text{O}_4$  filled rigid PU foams prepared at 4, 8, 16, 32, 40 and 50 wt.% for a magnification of X50

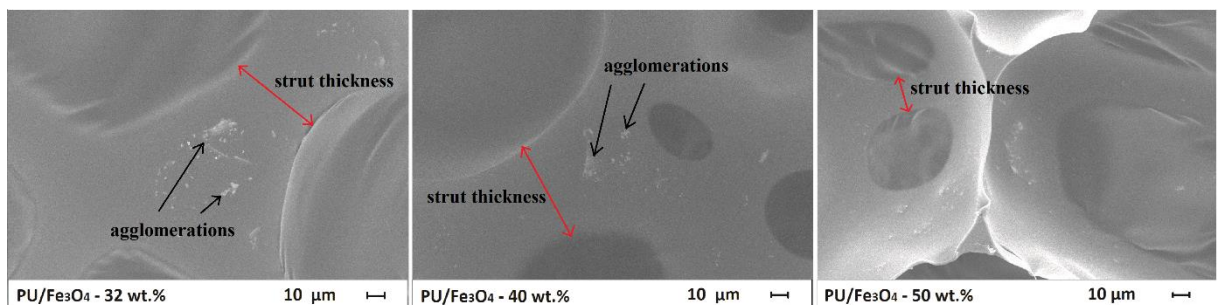


**Figure 3.** SEM images obtained for  $\text{Fe}_3\text{O}_4$  filled rigid PU foams prepared at 32, 40 and 50 wt.% for a magnification of X500

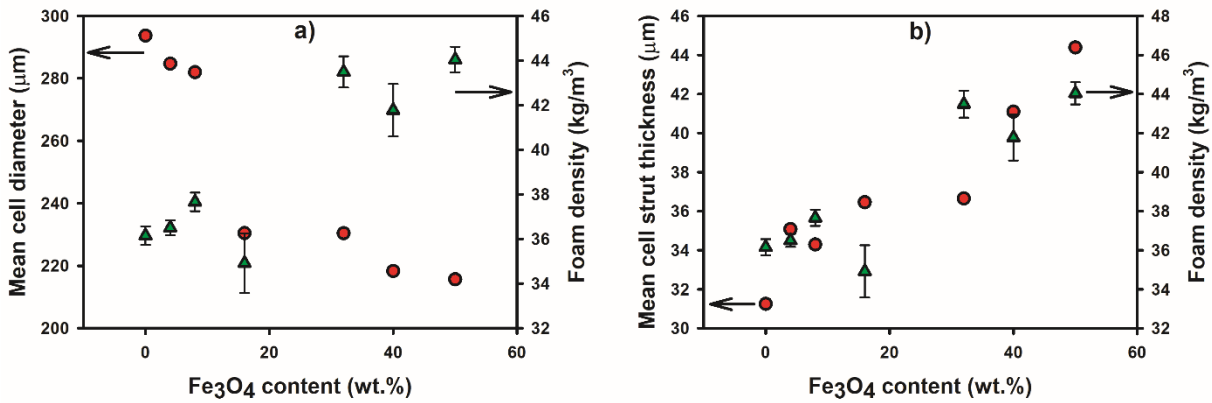


Figure 4. Evolution of the a) Mean cell diameter and b) Mean cell strut thickness of unfilled and Fe<sub>3</sub>O<sub>4</sub> filled rigid PU foams with increasing filler content

Table 1. Foam density, mean cell diameter and mean strut thickness of unfilled and Fe<sub>3</sub>O<sub>4</sub> filled rigid PU foams

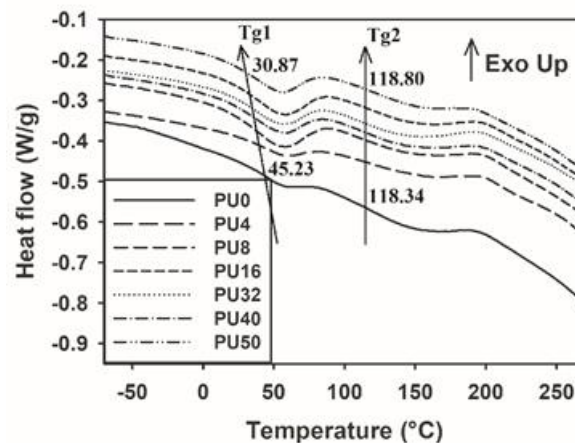
PU/Fe <sub>3</sub> O <sub>4</sub> foams	Foam density (kg/m <sup>3</sup> )	Mean cell diameter (µm)	Mean strut thickness (µm)
PU0	35.41 ± 1.33	294	31
PU4	37.56 ± 1.85	285	35
PU8	37.66 ± 0.41	282	34
PU16	36.00 ± 2.30	231	36
PU32	43.49 ± 0.70	231	37
PU40	41.77 ± 1.17	218	41
PU50	44.04 ± 0.57	215	44

### 3.2. Effect of filler concentration on the thermal transitions of rigid PU/Fe<sub>3</sub>O<sub>4</sub> foam nanocomposites

Figure 5 represents the DSC thermograms obtained for rigid PU/Fe<sub>3</sub>O<sub>4</sub> foam nanocomposites prepared at various filler amount (0, 4, 8, 16, 32, 40 and 50wt.%). From these graphs, two main transitions can be seen: the glass transitions of soft and hard segments of magnetite filled rigid PU foams (Tg1 and Tg2). The first transition represents the soft segments and was determined from the inflection point at the 0-50°C temperature domain whereas the second transition illustrates the hard segments and in the same way was obtained from the inflection point at the 75-150°C temperature area. Tg1 and Tg2 values were gathered in Table 2. From these results, as the magnetite content rises a visible diminution by 32% of Tg1 appears in the case of soft segments when Tg2 representing hard segments remains constant. The drop of the glass transition value for soft segments is probably due to the disorganization of entanglement meshes present in the PU matrix caused by the magnetite particles (Gu, et al., 2014). From Figure 5, it can also be observed that the gap between Tg1 and Tg2 is increasing with increasing the filler content. This behavior can be explained by the notable separation of soft and hard segments in the PU system as the magnetite amount rises (Ma, et al., 2019).

**Table 2.** Glass transition temperatures Tg1 and Tg2 of unfilled and Fe<sub>3</sub>O<sub>4</sub> filled rigid PU foams

PU/Fe <sub>3</sub> O <sub>4</sub> foams	Tg <sub>1</sub> (°C)	Tg <sub>2</sub> (°C)
PU0	45.23	118.34
PU4	38.88	119.11
PU8	36.58	119.81
PU16	35.15	118.13
PU32	33.53	118.19
PU40	31.89	118.79
PU50	30.87	118.80

**Figure 5.** DSC traces obtained for unfilled PU foam and Fe<sub>3</sub>O<sub>4</sub> filled rigid PU foams

### 3.3. Effect of filler concentration on the thermal conductivity of rigid PU/Fe<sub>3</sub>O<sub>4</sub> foam nanocomposites

The thermal conductivity results obtained for rigid PU/Fe<sub>3</sub>O<sub>4</sub> foam nanocomposites prepared at different concentrations of magnetite (0, 4, 8, 16, 32, 40 and 50wt.%) are presented on Figure 6. The results exhibit a slight increase from 0.02431W/m.K to 0.02648W/m.K for an optimum rise obtained in the case of a filler content of 4wt.%. Then, a decrease and a stabilization of the thermal conductivity can be observed. This behavior can be explained by the percolation threshold theory where a critical value is reached when a continuous pathway is produced by the fillers into the polymer matrix allowing an optimum thermal conductivity of the prepared rigid PU foam nanocomposites. In addition, the cell size of PU foams is a significant parameter which impact the thermal conductivity of these materials. In the literature, smaller cell size is related with lower thermal conductivity (Chen, et al., 2013; Lee, et al., 2016). The thermal conductivity of PU foams is the result of conduction by cell walls, convection, by gas blowing within cells and heat radiating across cells (Almanza, et al., 2000; Kang, et al., 2010). As a result, in this study, a decrease of the thermal conductivity is observed due to the decrease of the mean cell diameters with the increase of the Fe<sub>3</sub>O<sub>4</sub> content. This result shows a thermal insulating effect of magnetite particles. In this work, the decrease of the thermal conductivity of rigid PU/Fe<sub>3</sub>O<sub>4</sub> foam nanocomposites allows their application in construction and other industrial sectors requiring improved thermal insulating properties such as their use in refrigerators.

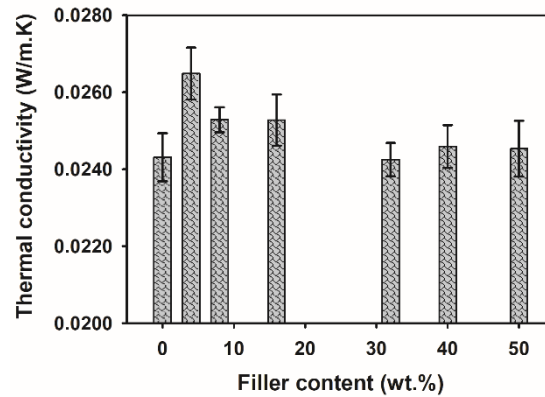


**Figure 6.** Thermal conductivity of un-filled and Fe<sub>3</sub>O<sub>4</sub> filled rigid PU foams prepared with various magnetite content

### 3.4. Effect of filler concentration on the electrical conductivity of rigid PU/Fe<sub>3</sub>O<sub>4</sub> foam nanocomposites

Figure 7 shows the electrical conductivity of rigid PU/Fe<sub>3</sub>O<sub>4</sub> foam nanocomposites prepared at different filler amount (0, 4, 8, 16, 32, 40 and 50wt.%). From Figure 7, a sharp increase up to 4wt.% of filler and then a stabilization of the electrical conductivity between 0 and 50wt.% of magnetite in polyol can be seen. Then, a rise by 17% can be observed as the iron (II, III) oxide amount reaches 50wt.%. As previously presented in the case of the thermal conductivity, this behavior can be explained by the percolation theory mainly reported in the literature (Akkoyun & Akkoyun, 2019). A critical concentration of magnetite can be determined as 4wt.% representing the electrical percolation threshold from which the magnetite particles forms an uninterrupted network in the PU matrix. The improved electrical conductivity of these materials as the Fe<sub>3</sub>O<sub>4</sub> content increases, allows their use in areas such as magnetic and electromagnetic wave absorption.

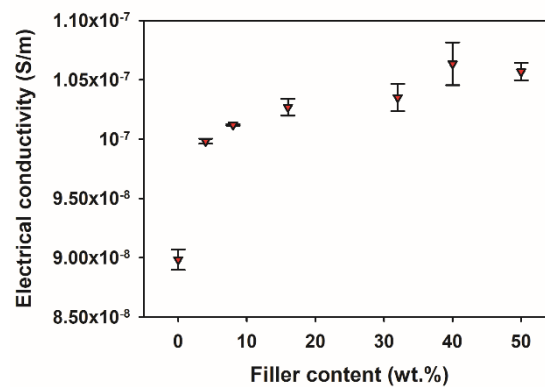


**Figure 7.** Electrical conductivity of un-filled and Fe<sub>3</sub>O<sub>4</sub> filled rigid PU foams prepared with various magnetite content

## 4. CONCLUSIONS

The electrical and thermal conductivities, microstructure and thermal transition properties of rigid PU/Fe<sub>3</sub>O<sub>4</sub> foam nanocomposites prepared at various filler content were investigated. A drop of the average cell diameter by 27% was obtained as the filler concentration increases up to 50wt.%. The thermal transition results showed a visible decrease by 32% of the glass transition temperature appears in the case of soft segments when the glass transition temperature representing hard segments remains constant. Results of the electrical and thermal conductivities revealed the presence of a percolation threshold which

is determined as 4wt.% for each case. When a thermal insulating effect of magnetite particles can be concluded, the electrical conductivity of rigid PU/Fe<sub>3</sub>O<sub>4</sub> foam nanocomposites showed an important increase by 17% as the filler concentration rises up to 50wt.%. In this work, the decrease of the thermal conductivity of rigid PU/Fe<sub>3</sub>O<sub>4</sub> foam nanocomposites allows their application in construction and other industrial sectors requiring improved thermal insulating properties such as their use in refrigerators. At the same time, due to their improved electrical conductivity as the Fe<sub>3</sub>O<sub>4</sub> content increases, these materials can also be used in areas such as magnetic and electromagnetic wave absorption.

## ACKNOWLEDGEMENT

Kimteks/Turkey is gratefully acknowledged for the supply of polyol and isocyanate.

## REFERENCES

- Akkoyun, M., Akkoyun, S., 2019 "Blast furnace slag or fly ash filled rigid polyurethane composite foams: A comprehensive investigation", *Journal of Applied Polymer Science*, Vol. 136, pp. 47433.
- Akkoyun, M., Suvaci, E., 2016 "Effects of TiO<sub>2</sub>, ZnO, and Fe<sub>3</sub>O<sub>4</sub> nanofillers on rheological behavior, microstructure, and reaction kinetics of rigid polyurethane foams", *Journal of Applied Polymer Science*, Vol. 133, pp. 43658.
- Alavi Nikje, M. M., Akbar, R., Ghavidel, R., Vakili, M., 2015a, "Preparation and Characterization of Magnetic Rigid Polyurethane Foam Reinforced with Dipodal Silane Iron Oxide Nanoparticles Fe<sub>3</sub>O<sub>4</sub>@APTS/GPTS", *Cellular Polymers*, Vol. 34, No. 3, pp. 137-156.
- Alavi Nikje, M. M., Farahmand Nejad, M. A., Shabani, K., Haghshenas, M., 2013, "Preparation of magnetic polyurethane rigid foam nanocomposites", *Colloid and Polymer Science*, Vol. 291, pp. 903-909.
- Alavi Nikje, M. M., Noruzian, M., Moghaddam, T. S., 2015b, "Novel Polyurethane Rigid Foam/Organically Modified Iron oxide Nanocomposites", *Polymer Composites*, Vol. 38, No. 5, pp. 877-883.
- Almanza, O. A., Rodriguez-Perez, M. A., de Saja, J. A., 2000, "Prediction of the Radiation Term in the Thermal Conductivity of Crosslinked Closed Cell Polyolefin Foams", *Journal of Polymer Science: Part B: Polymer Physics*, Vol. 38, pp. 993-1004.
- Baferani, A. H., Katbab, A. A., Ohadi, A. R., 2017, "The role of sonication time upon acoustic wave absorption efficiency, microstructure, and viscoelastic behavior of flexible polyurethane/CNT nanocomposite foam" *European Polymer Journal*, Vol. 90, pp. 383-391.
- Caba, V., Borgese, L., Agnelli, S., Depero, L. E., 2019, "A green and simple process to develop conductive polyurethane foams for biomedical applications", *International Journal of Polymeric Materials and Polymeric Biomaterials*, Vol. 68, pp. 126-133.
- Chattopadhyay, D. K., Webster, D. C., 2009, "Thermal stability and flame retardancy of polyurethanes", *Progress in Polymer Science*, Vol. 34, No. 10, pp. 1068-1133.
- Chen, L., Rende, D., Schadler, L. S., Ozisik, R., 2013, "Polymer nanocomposite foams", *Journal of Materials Chemistry A*, Vol. 1, pp. 3837.
- Chen, Y., Huang, X., Gong, Z., Xu, C., Mou, W., 2017, "Fabrication of High Performance Magnetic Rubber from NBR and Fe<sub>3</sub>O<sub>4</sub> via in Situ Compatibilization with Zinc Dimethacrylate", *Industrial & Engineering Chemistry Research*, Vol. 56, No. 1, pp. 183-190.
- Ghariniyat, P., Leung, S. N., 2018, "Development of thermally conductive thermoplastic polyurethane composite foams via CO<sub>2</sub> foaming-assisted filler networking", *Composites Part B: Engineering*, Vol. 143, pp. 9-18.
- Gu, S.-Y., Liu, L.-L., Yan, B., 2014, "Effects of ionic solvent-free carbon nanotube nanofluid on the properties of polyurethane thermoplastic elastomer", *Journal of Polymer Research*, Vol. 21, pp. 356.
- Han, X., Koelling, K., Tomasko, D., Lee, L., 2002, "Continuous microcellular polystyrene foam extrusion with supercritical CO<sub>2</sub>", *Polymer Engineering and Science*, Vol. 42, pp. 2094.
- Ibeh, C. C., Bubacz, M., 2008, "Current Trends in Nanocomposite Foams", *Journal of Cellular Plastics*, Vol. 44, No. 6, pp. 493-515.

- Kang, M. J., Kim, Y. H., Park, G. P., Han, M. S., Kim, W. N., Park, S. D., 2010, "Liquid nucleating additives for improving thermal insulating properties and mechanical strength of polyisocyanurate foams", *Journal of Materials Science*, Vol. 45, pp. 5412–5419.
- Król, P., Król, B., Pielichowska, K., Špírková, M., 2015, "Composites prepared from the waterborne polyurethane cationomers-modified graphene. Part I. Synthesis, structure, and physicochemical properties", *Colloid and Polymer Science*, Vol. 293, pp. 421–431.
- Lee, L. J., Zeng, C., Cao, X., Han, X., Shen, J., Xu, G., 2005, "Polymer nanocomposite foams", *Composites Science and Technology*, Vol. 65, pp. 344–2363.
- Lee, S.-T., Ramesh, N. S., 2004, "Polymeric foams: mechanisms and materials", Boca Raton: CRC Press.
- Lee, Y., Jang, M. G., Choi, K. H., Han, C., Kim, W. N., 2016, "Liquid-type nucleating agent for improving thermal insulating properties of rigid polyurethane foams by HFC-365mfc as a blowing agent", *Journal of Applied Polymer Science*, Vol. 133, pp. 43557.
- Lorusso, C., Vergaro, V., Conciauro, F., Ciccarella, G., Congedo, P., 2017, "Thermal and mechanical performance of rigid polyurethane foam added with commercial nanoparticles", *Nanomaterials and Nanotechnology*, Vol. 7, pp. 1–9.
- Ma, X., Shi, C., Huang, X., Liu, Y., Wei, Y., 2019, "Effect of natural melanin nanoparticles on a self-healing cross-linked polyurethane", *Polymer Journal*, Vol. 51, pp. 547-558.
- Moghaddam, S. T., Naimi-Jamal, R. M., 2018, "Reinforced magnetic polyurethane rigid (PUR) foam nanocomposites and investigation of thermal, mechanical, and sound absorption properties", *Journal of Thermoplastic Composite Materials*, Vol. 32, No. 9, pp. 1224-1241.
- Paciorek-Sadowska, J., Borowicz, M., Isbrandt, M., Czuprynski, B., Apiecioneck, L., 2019, "The Use of Waste from the Production of Rapeseed Oil for Obtaining of New Polyurethane Composites", *Polymers*, Vol. 11, pp. 1431.
- Patcharapon, S., Kalman, M., Timea, L.-K., Csaba, K., 2018, "Polyurethane elastomers with improved thermal conductivity part I: elaborating matrix material for thermal conductive composites", *International Journal of Mechanical and Production Engineering*, Vol. 6, pp. 2320-2092.
- Pillai, P. K., Li, S., Bouzidi, L., Narine, S. S., 2015, "Metathesized palm oil polyol for the preparation of improved bio-based rigid and flexible polyurethane foams", *Industrial Crops and Products*, Vol. 83, pp. 568-576.
- Saha, M. C., Kabir, M. E., Jeelani, S., 2008, "Enhancement in thermal and mechanical properties of polyurethane foam infused with nanoparticles", *Materials Science and Engineering: A*, Vol. 479, No. 1-2, pp. 213-222.
- Saha, M. C., Mahfuz, H., Chakravarty, U. K., Uddin, M., Kabir, M. E., Jeelani, S., 2005, "Effect of density, microstructure, and strain rate on compression behavior of polymeric foams", *Materials Science and Engineering*, Vol. 406, pp. 328–336.
- Sattar, R., Kausar, A., Siddiq, M., 2015, "Advances in thermoplastic polyurethane composites reinforced with carbon nanotubes and carbon nanofibers: A review", *Journal of Plastic Film & Sheeting*, Vol. 31, No. 2, pp. 86–224.
- Silva, A. M., Pereira, I. M., Silva, T. I., da Silva, M. R., Rocha, R. A., Silva, M. C., 2020, "Magnetic foams from polyurethane and magnetite applied as attenuators of electromagnetic radiation in X band", *Journal of Applied Polymer Science*, pp. 49629.
- Usman, A., Zia, K. M., Zuber, M., Tabasum, S., Rehman, S., Zia, F., 2016, "Chitin and chitosan based polyurethanes: A review of recent advances and prospective biomedical applications", *International Journal of Biological Macromolecules*, Vol. 86, pp. 630–645.
- Wilkes, G. L., Wildnauer, R., 1975, "Kinetic behavior of the thermal and mechanical properties of segmented urethanes", *Journal of Applied Physics*, Vol. 46, pp. 4148.
- Zhang, G., Zhang, S., Qiu, J., Jiang, Z., Xing, H., Li, M., Tang, T., 2017, "Insight into the influence of OA-Fe<sub>3</sub>O<sub>4</sub> nanoparticles on the morphology and scCO<sub>2</sub> batch-foaming behavior of cocontinuous LLDPE/PS immiscible blends at semi-solid state", *Polymer*, Vol. 129, pp. 169-178.

- Zhou, L., Li, G., An, T., Li, Y., 2010, "Synthesis and characterization of novel magnetic Fe<sub>3</sub>O<sub>4</sub>/polyurethane foam composite applied to the carrier of immobilized microorganisms for wastewater treatment", *Research on Chemical Intermediates*, Vol. 36, pp. 277–288.
- Zou, H., Weder, C., Simon, Y. C., 2015, "Shape-Memory Polyurethane Nanocomposites with Single Layer or Bilayer Oleic Acid-Coated Fe<sub>3</sub>O<sub>4</sub> Nanoparticles", *Macromolecular Materials and Engineering*, Vol. 9, pp. 885-892.